Supporting Information

Visualization of Interfacial Electrostatic Complementarity Reveals Evolutionary Changes in SARS-CoV-2 RBD–ACE2 Interactions

Yosuke Muroya, Hiroki Ozono, and Takeshi Ishikawa*

Department of Chemistry, Biotechnology, and Chemical Engineering, Graduate School of Science and Engineering, Kagoshima University, 1-21-40 Korimoto, Kagoshima, Kagoshima 890-0065, Japan

Correspondence to: Takeshi Ishikawa (E-mail: ishi@cb.kagoshima-u.ac.jp)

Figure S1: Graphical representations of the complex structures of the 15 variants are shown in (A). A superimposed view of these 15 structures, aligned so that the hACE2 components overlap, is also provided in (B).

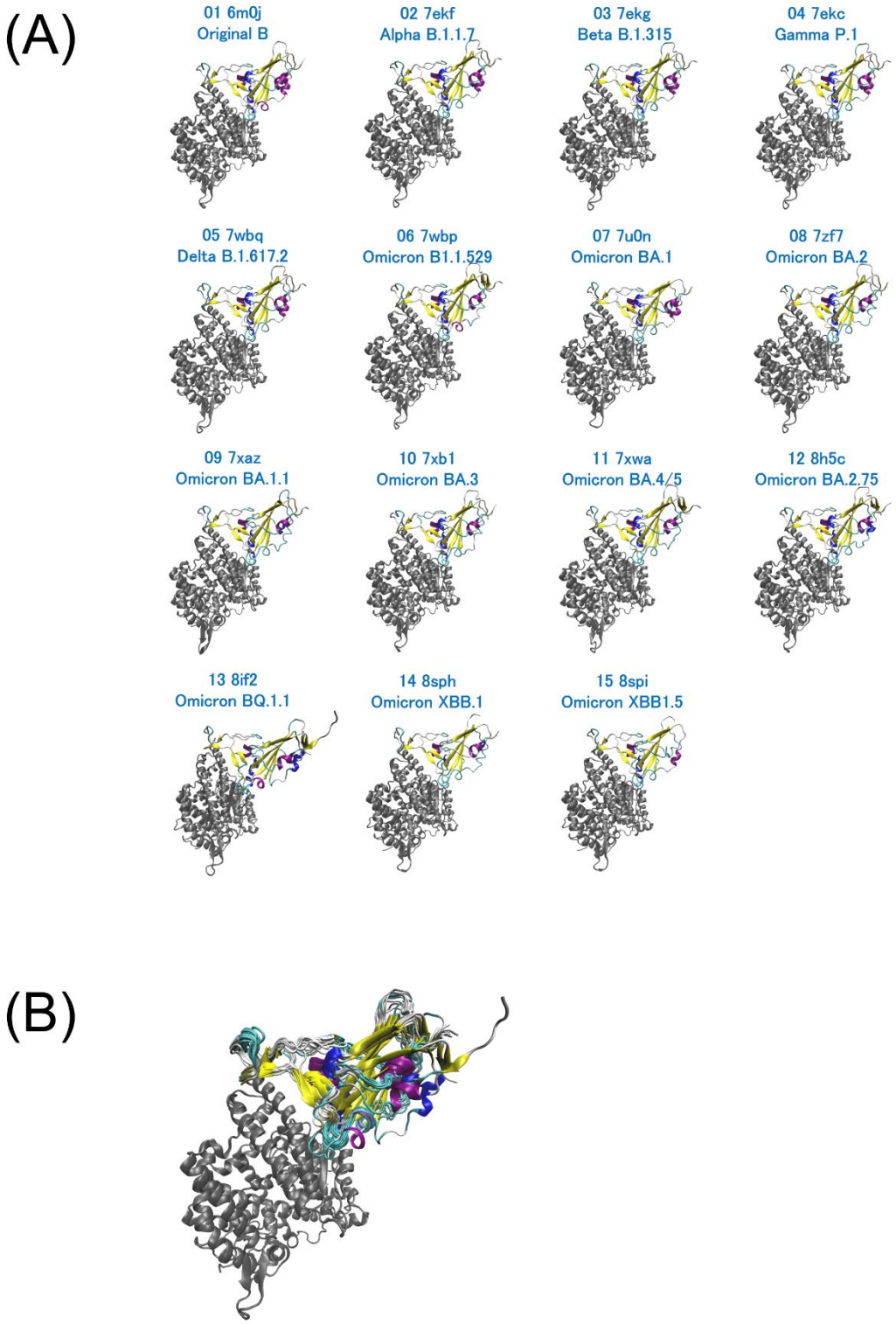

Figure S2: Alignment of the amino acid sequences of the RBDs from the 15 variants.

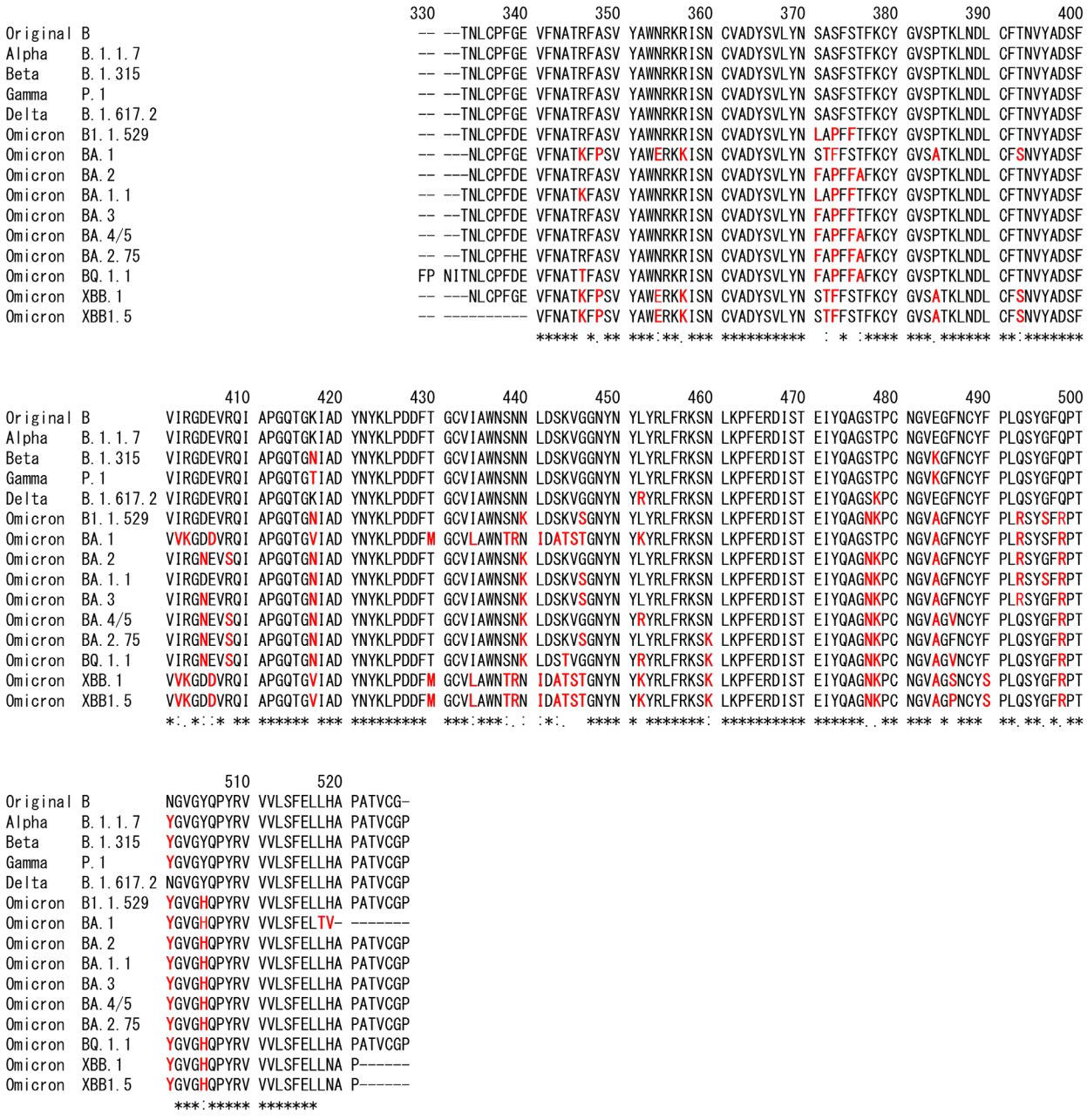

Figure S3: Visualization of the pESP at the CGCs for the complexes of the 15 variants. Results are provided for the cases without neutralization, with charge-removed neutralization, and constant-added neutralization. The R^- and D^- values are also provided.

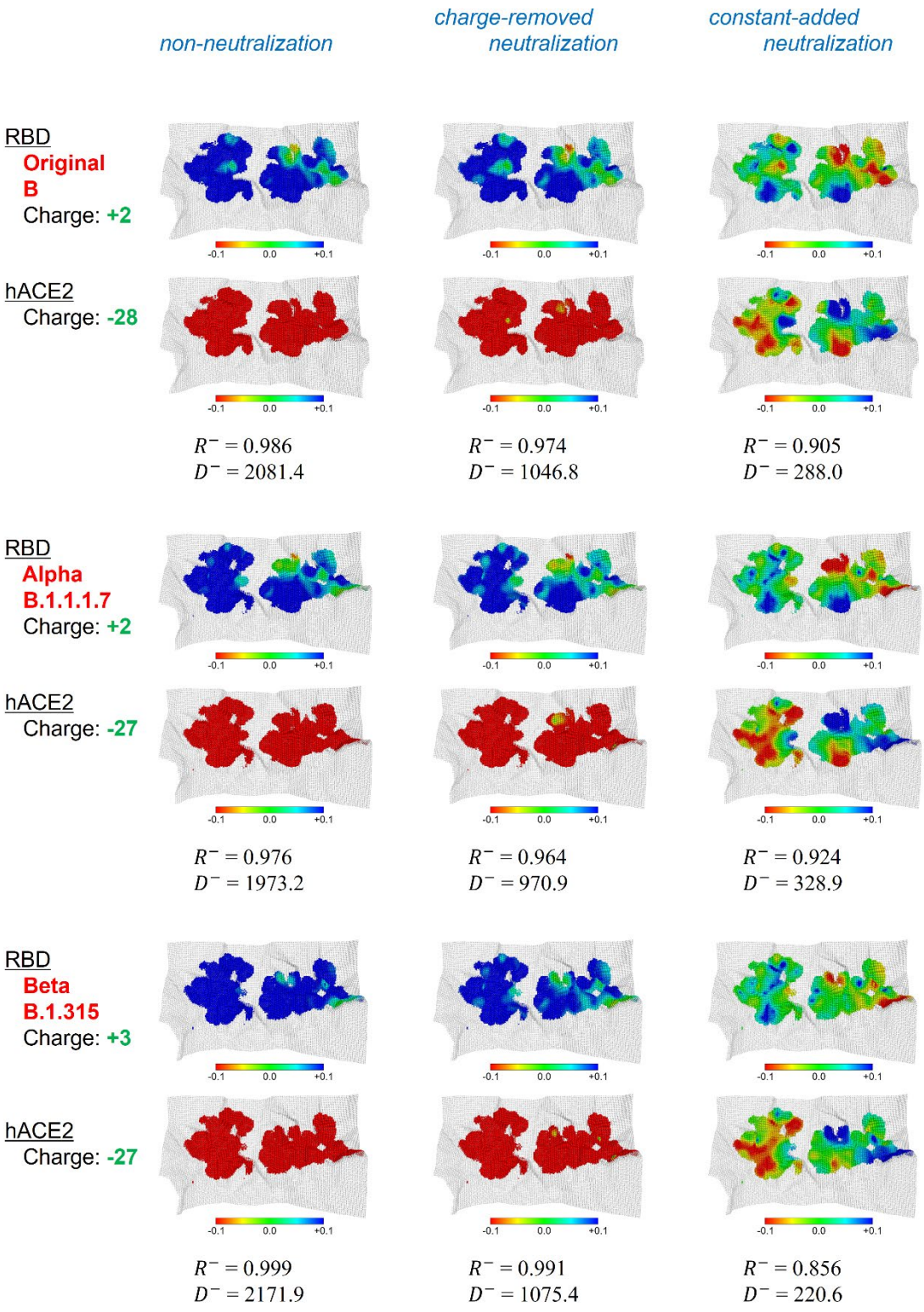

Figure S3 (continued)

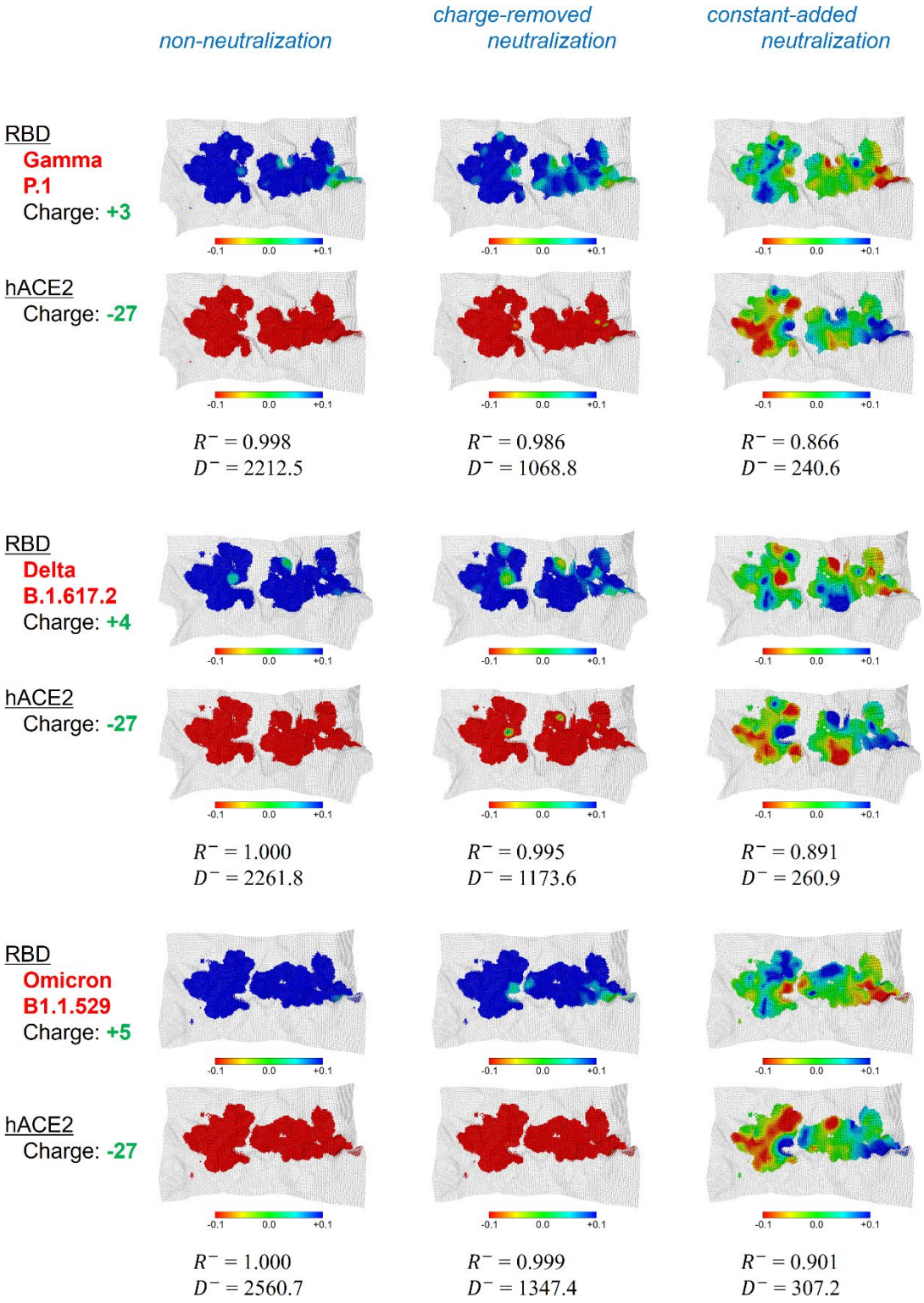

Figure S3 (continued)

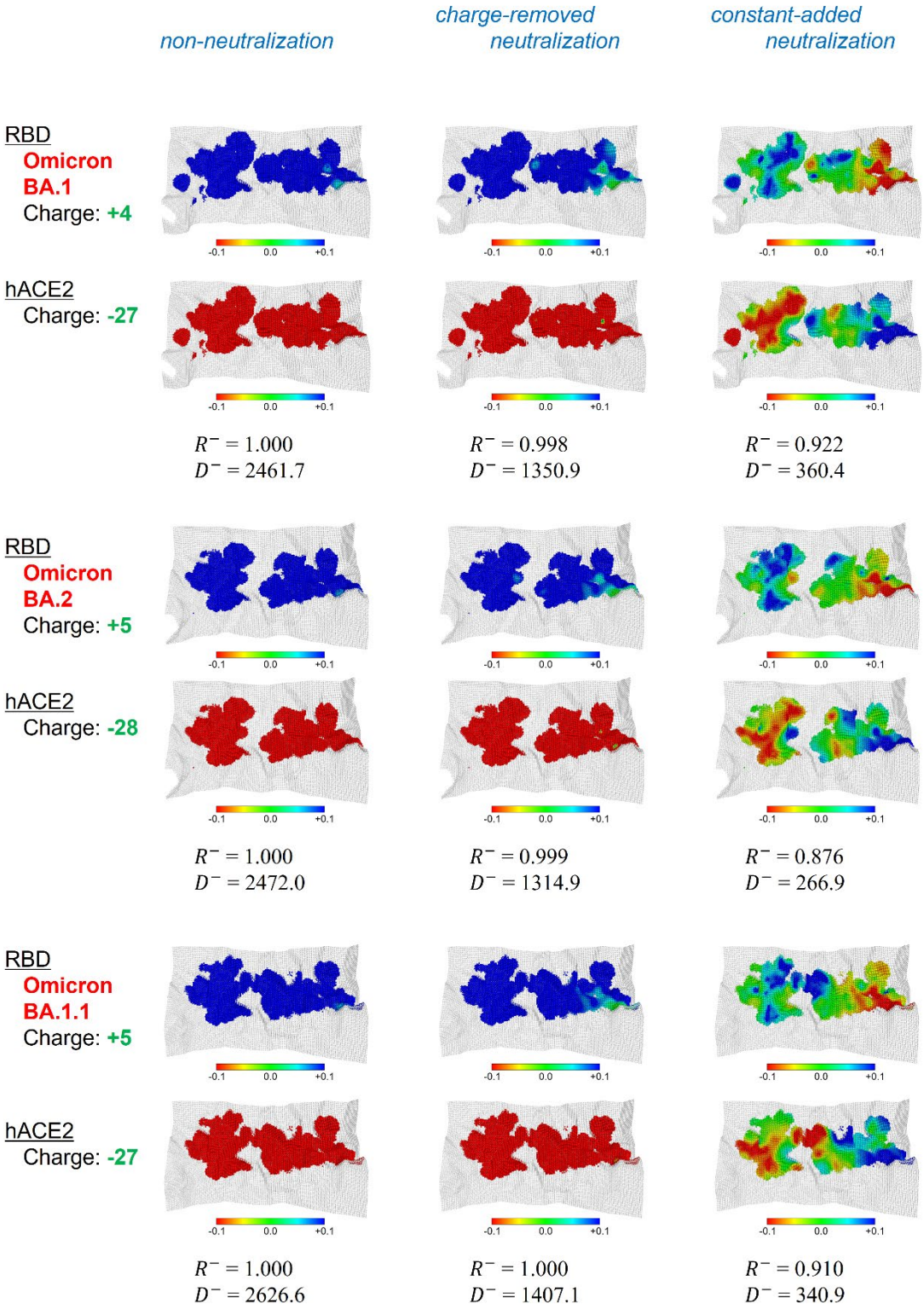

Figure S3 (continued):

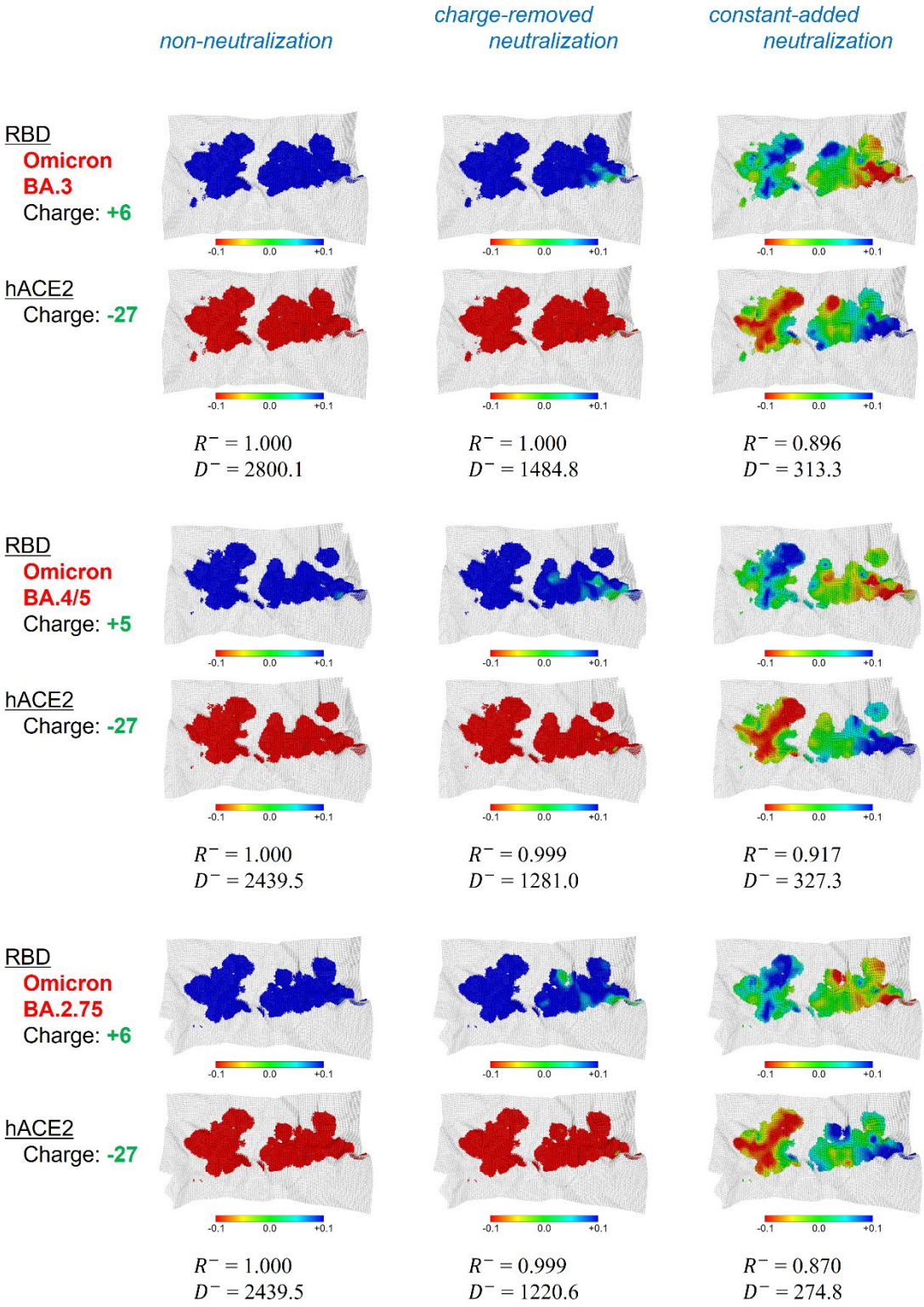

Figure S3 (continued):

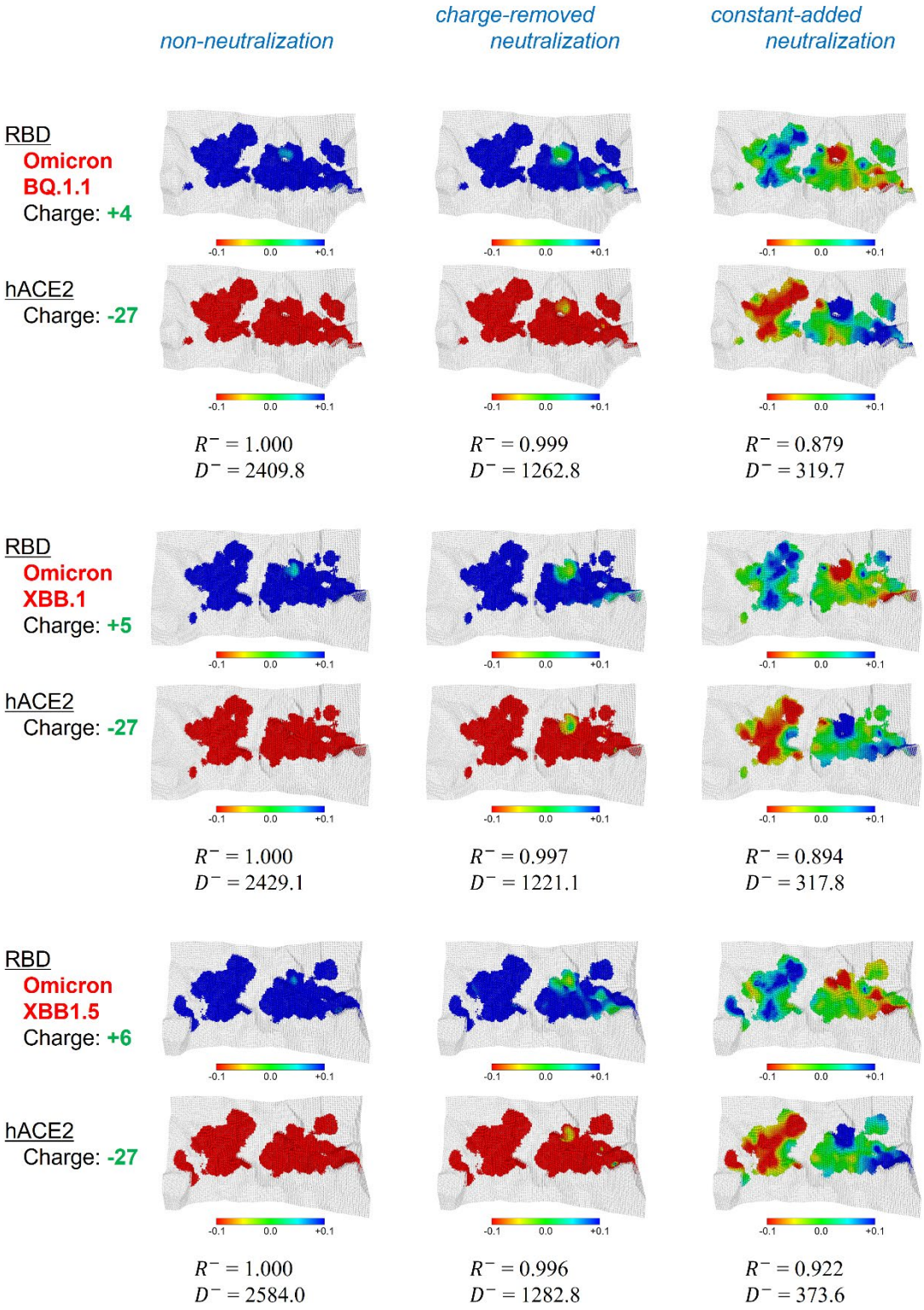

Figure S4: Visualization of the isolated protein's ESP at the CGCs for the 15 variants. Results are provided for the cases without neutralization, with charge-removed neutralization, and constant-added neutralization. The R^- and D^- values are also provided. Values in parentheses indicate the differences from the corresponding values of the pESP of the complexes.

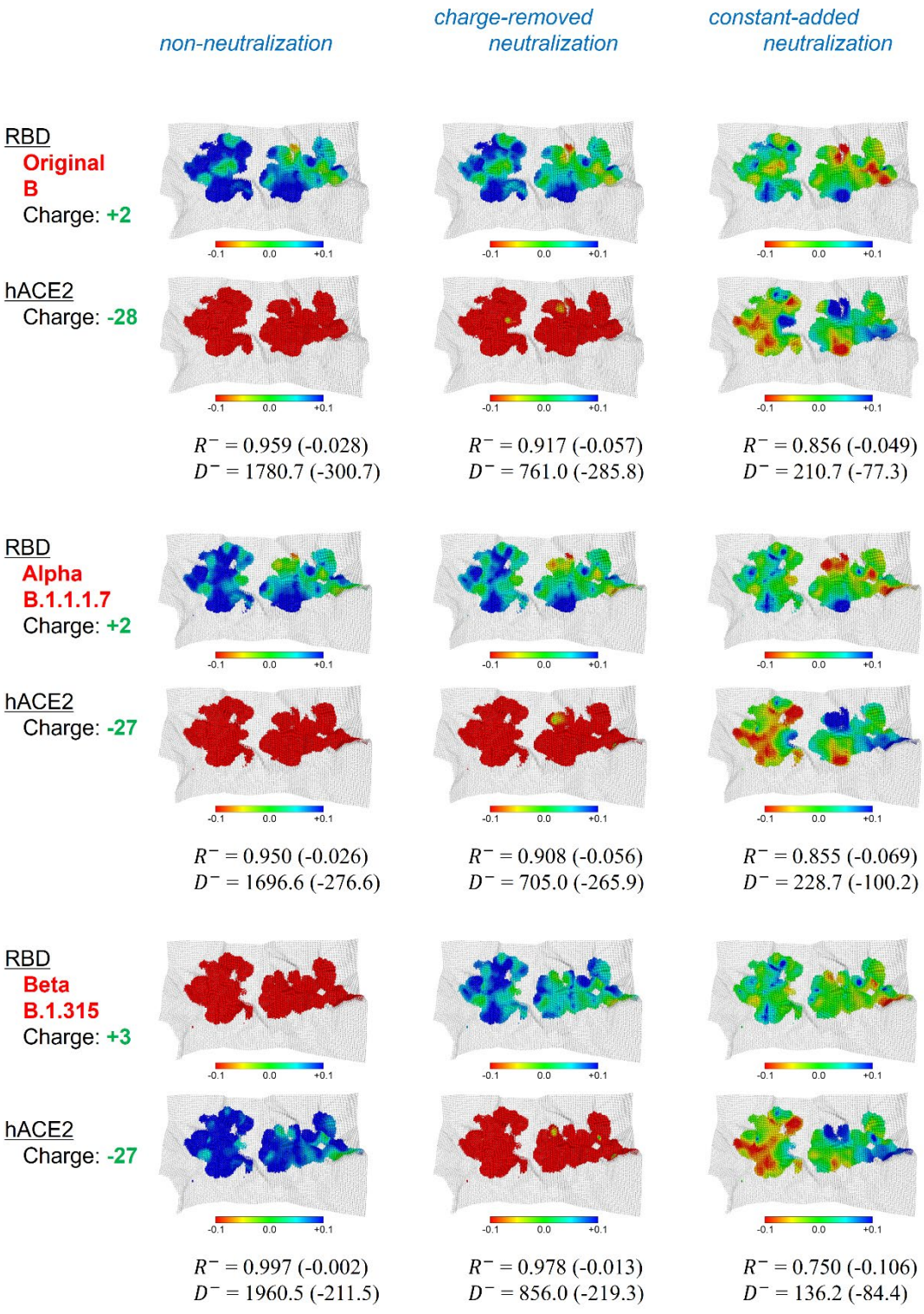

Figure S4(continued)

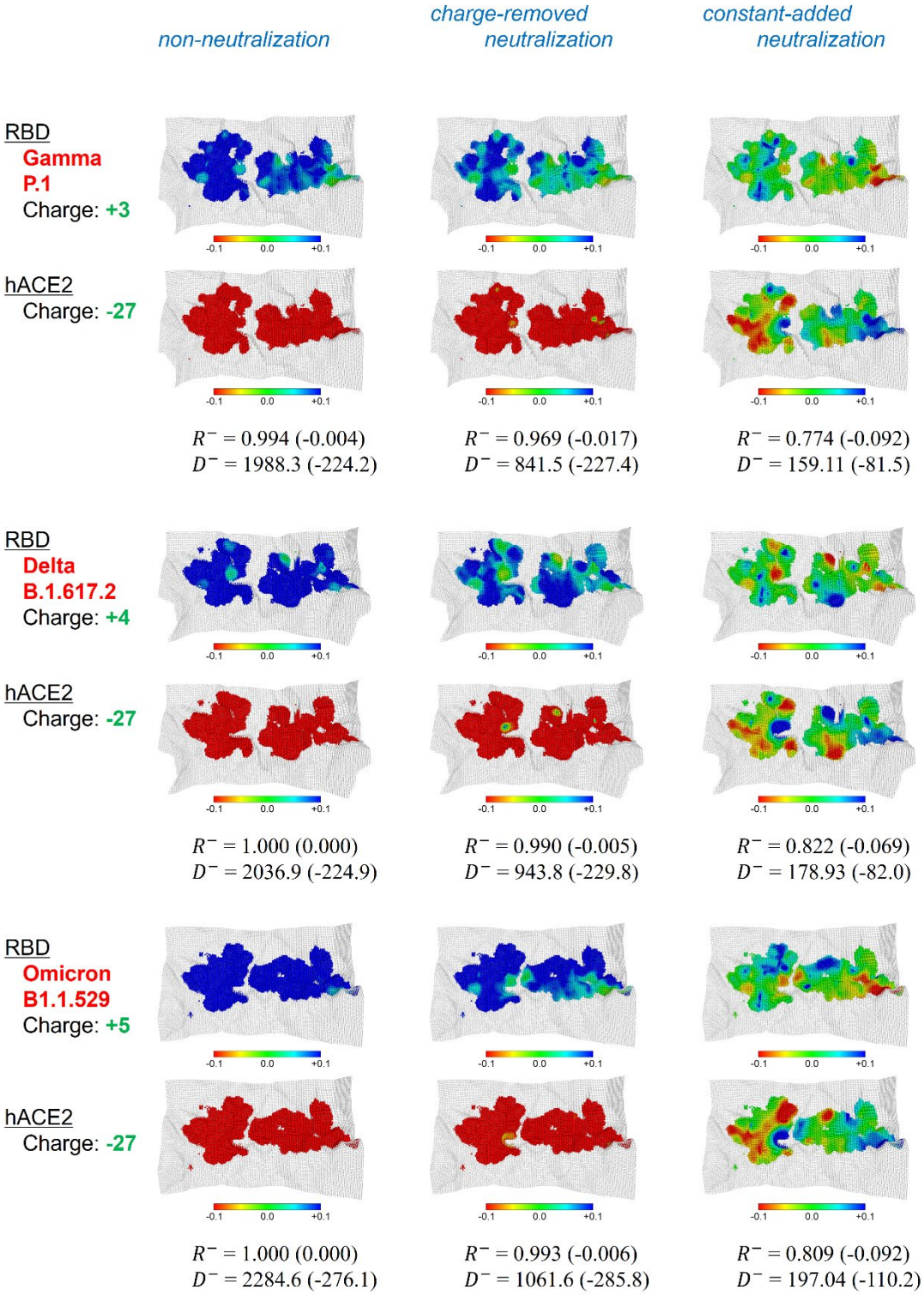

Figure S4(continued):

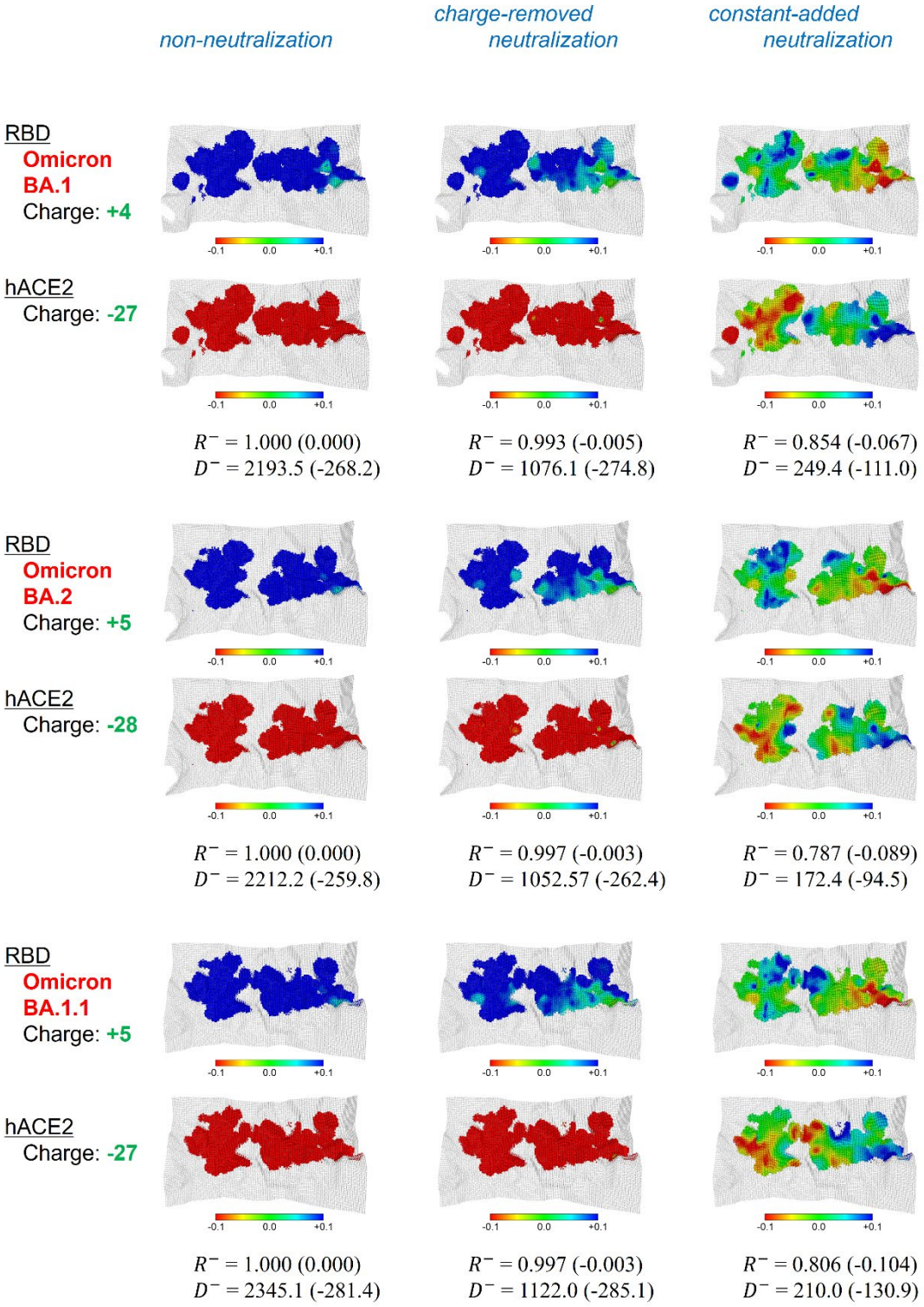

Figure S4(continued):

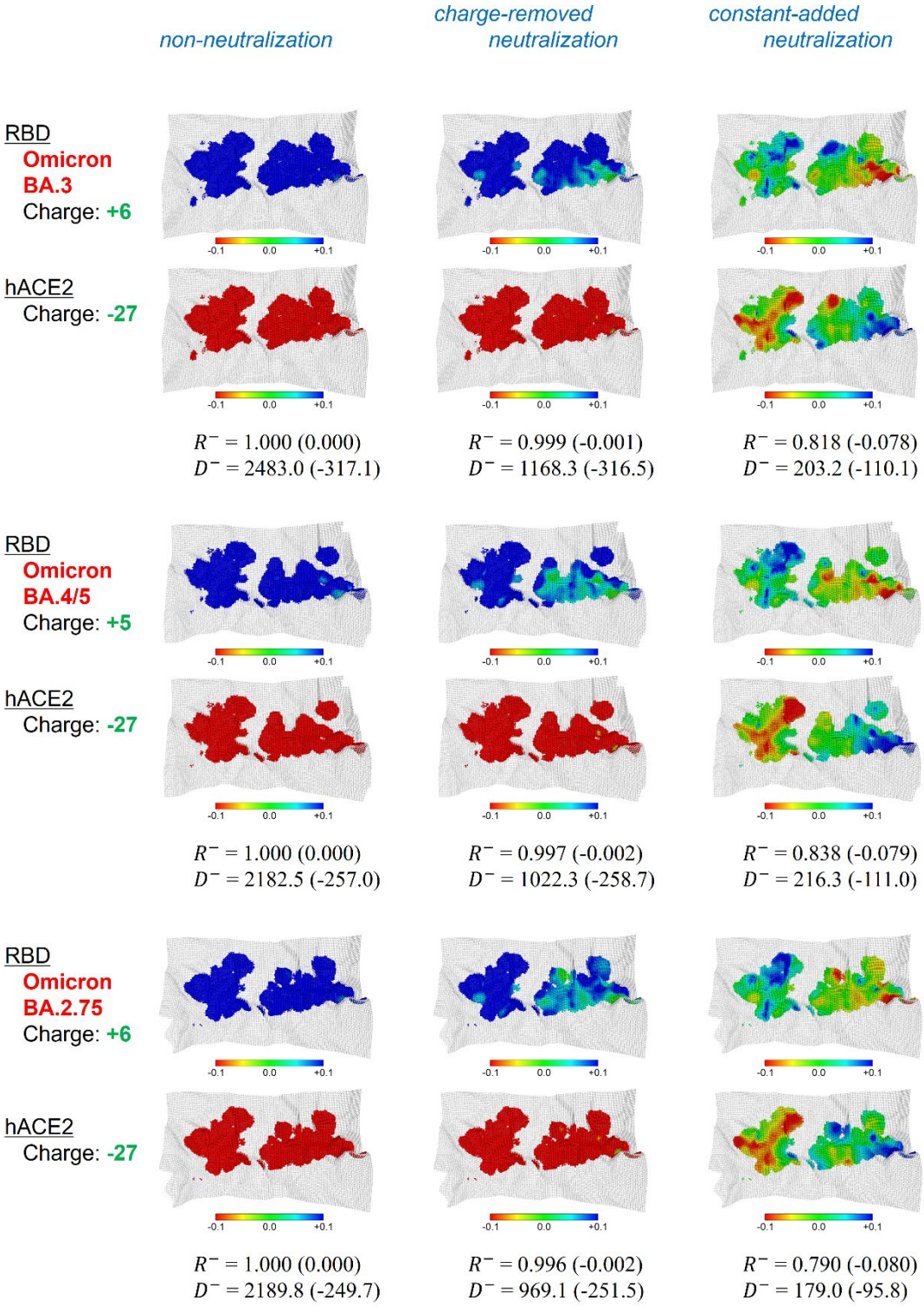

Figure S4(continued):

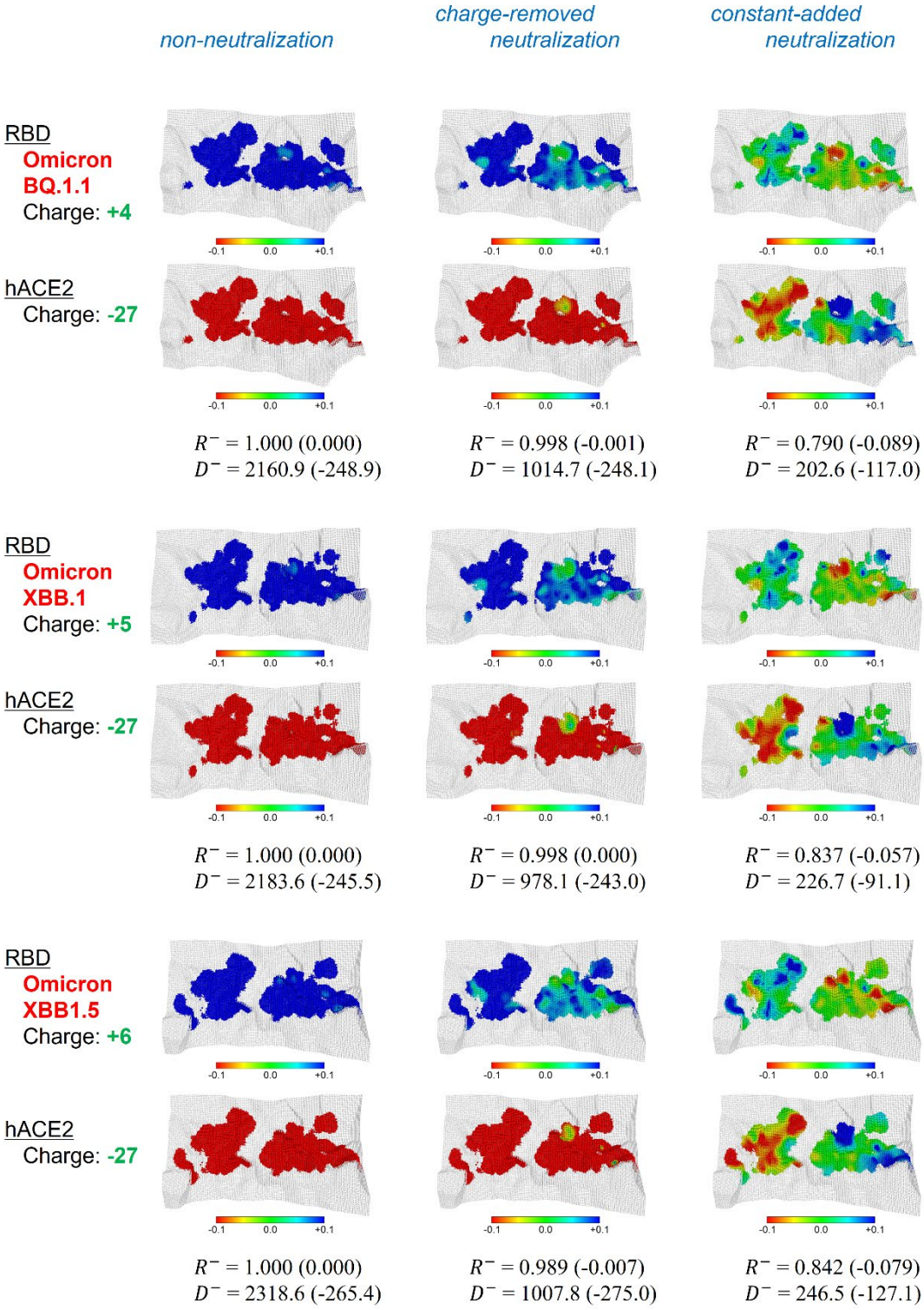

Figure S5: Visualization of the pEDN (i.e., the $\rho_i^A + \rho_i^B$) at the CGCs for the complexes of the 15 variants, along with the EDN of the corresponding isolated proteins. The ρ^+ values are also provided.

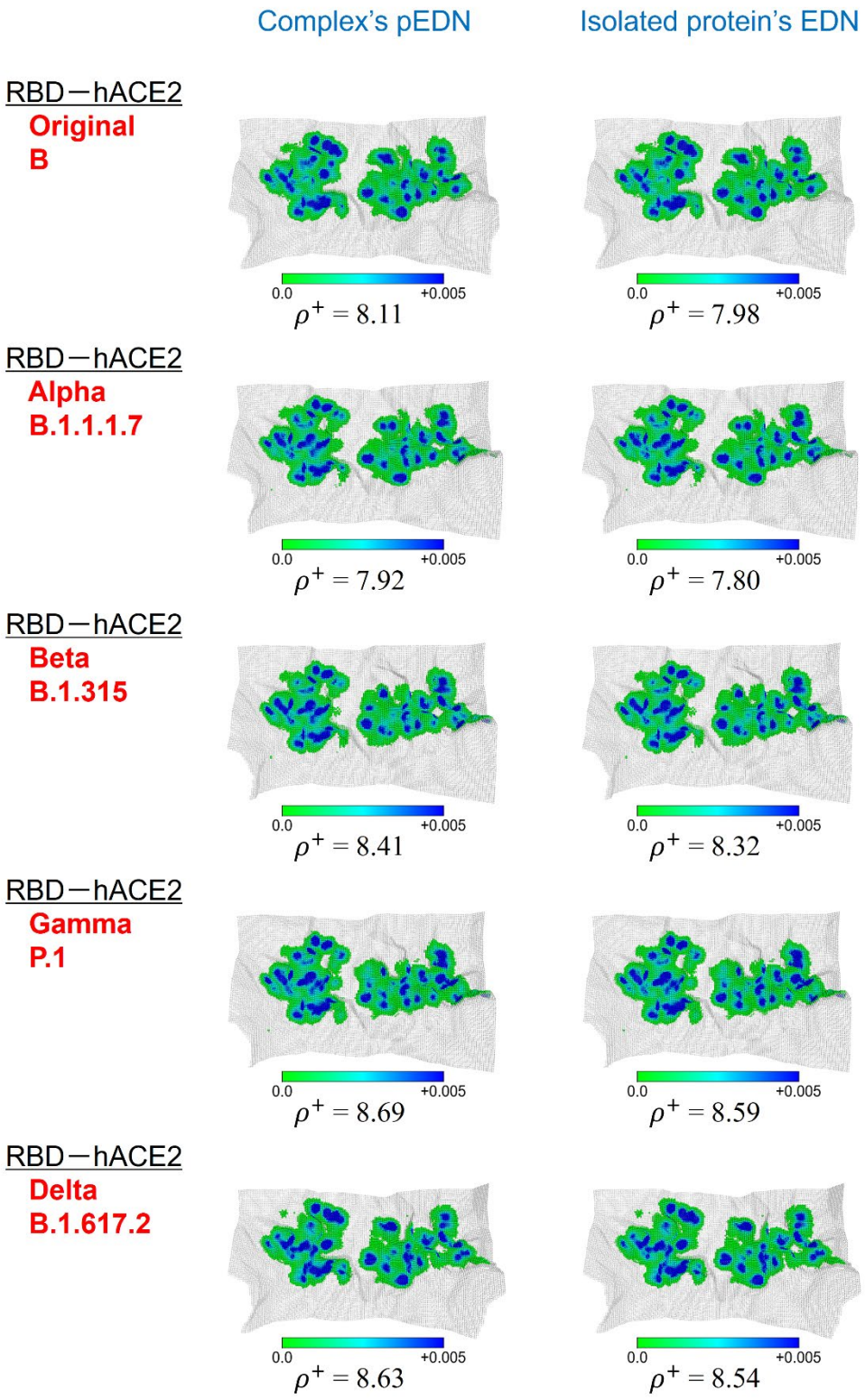

Figure S5(continued)

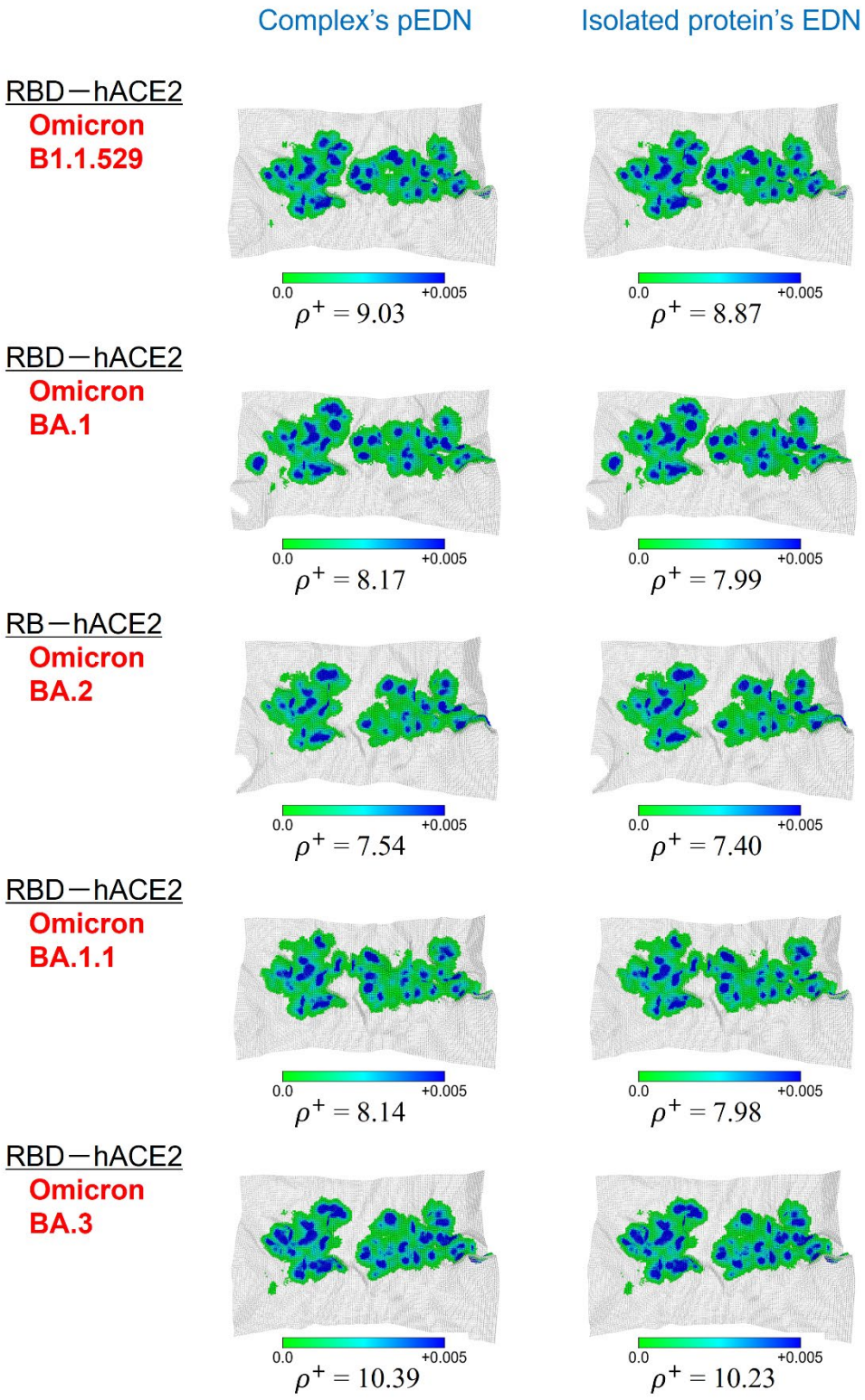

Figure S5(continued)

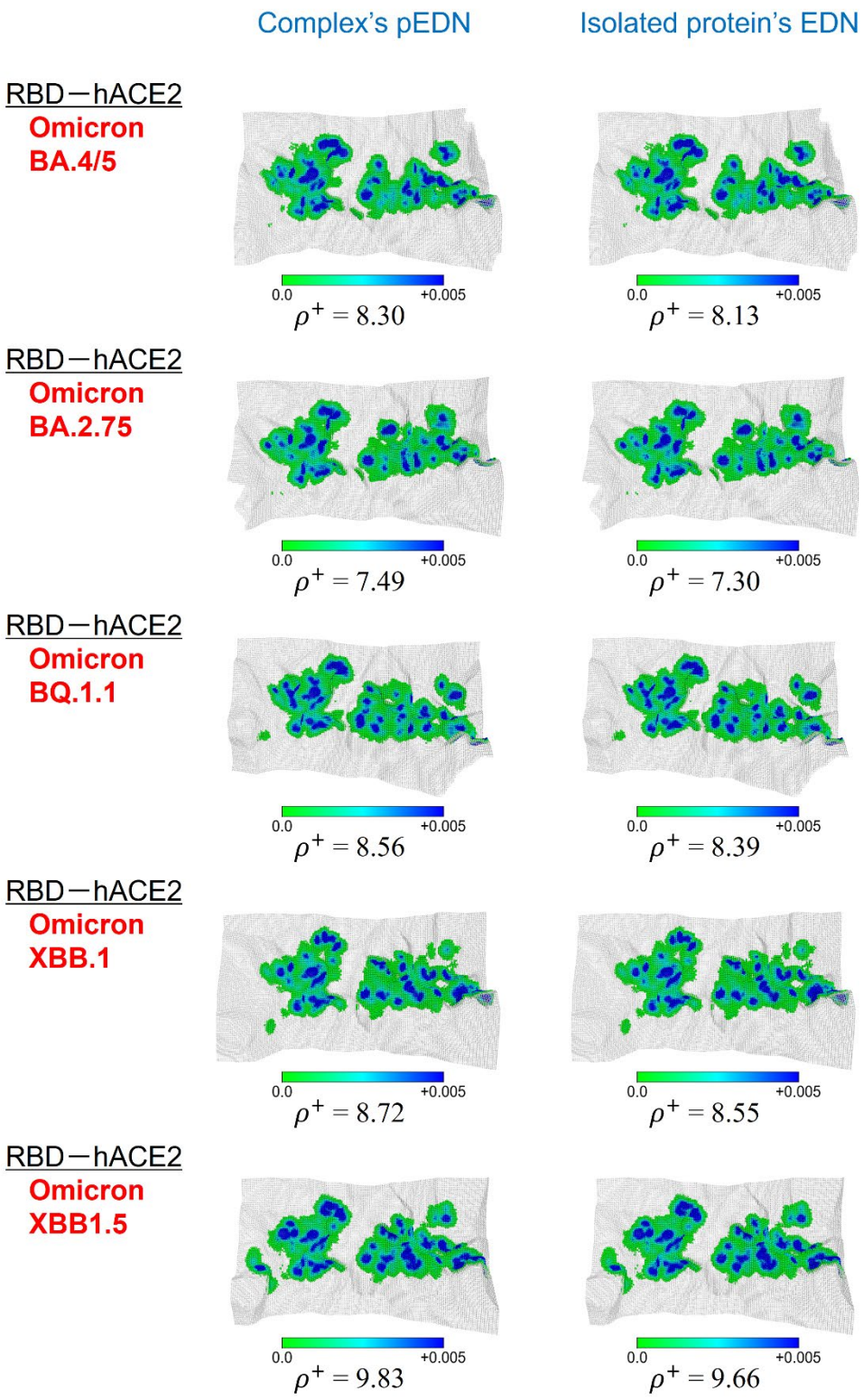

Figure S6: Visualization of the pESP of the RBDs after excluding the contributions of selected amino acids. Constant-added neutralization was applied. The R^- and D^- values are also provided.

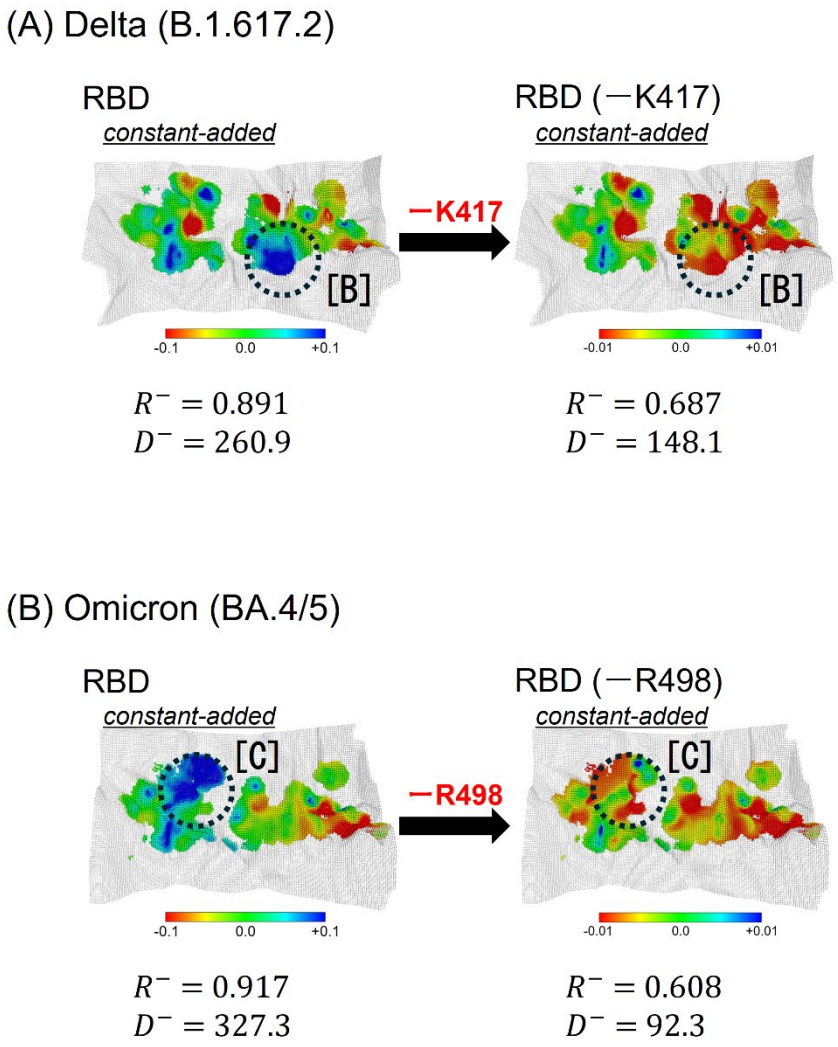

Figure S7: A scatter plot showing the correlation between the D^- values and the electrostatic interaction energies (ΔE^{HF}) obtained from the FMO calculations. Here, the D^- values with charge-removed neutralization. The detailed definition of ΔE^{HF} is described in previous paper [H. Ozono, et al., J. Phys. Chem. B, 2022, 126 (42), 8415].

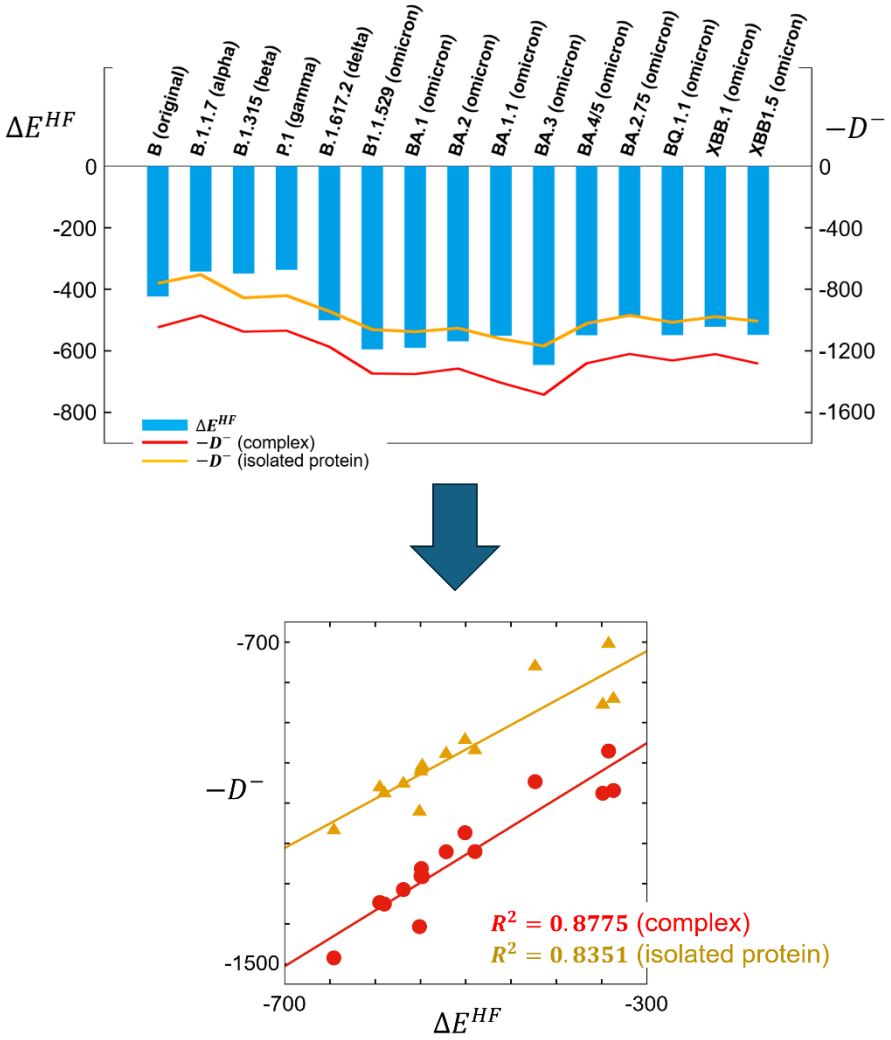

Figure S8: A scatter plot showing the correlation between the ρ^+ values and the total MP2 correlation energies (ΔE^{MP2}) obtained from the FMO calculations. The detailed definition of ΔE^{MP2} is described in previous paper [H. Ozono, et al., J. Phys. Chem. B, 2022, 126 (42), 8415].

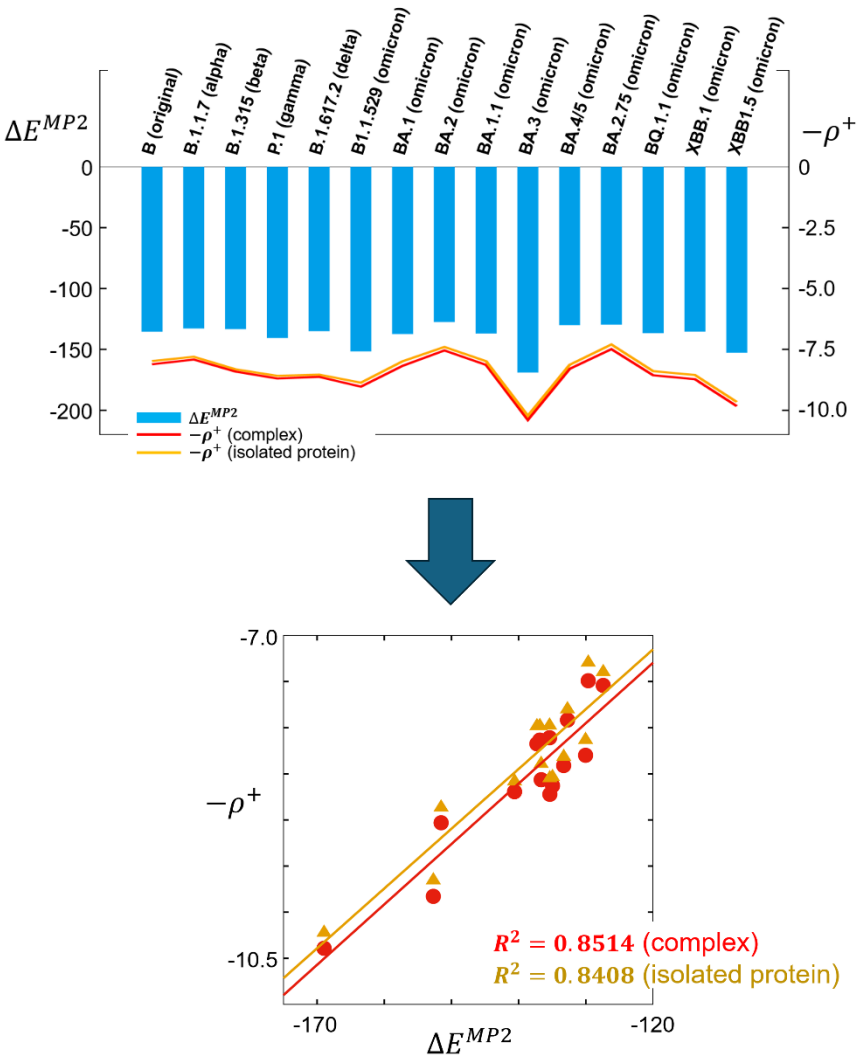

Figure S9: MP2 correlation energies of individual amino acid residues near the interface for the 15 complexes. These values were obtained from the IFIE analysis in the FMO method. Energies of the amino acids for the RBDs are shown on the left-hand side, and those for hACE2 are shown on the right-hand side. Amino acids highlighted in green indicate mutations from the original strain. Cysteine residues forming a disulfide bond were treated as a single fragment in our calculations; therefore, their energies are provided as combined values.

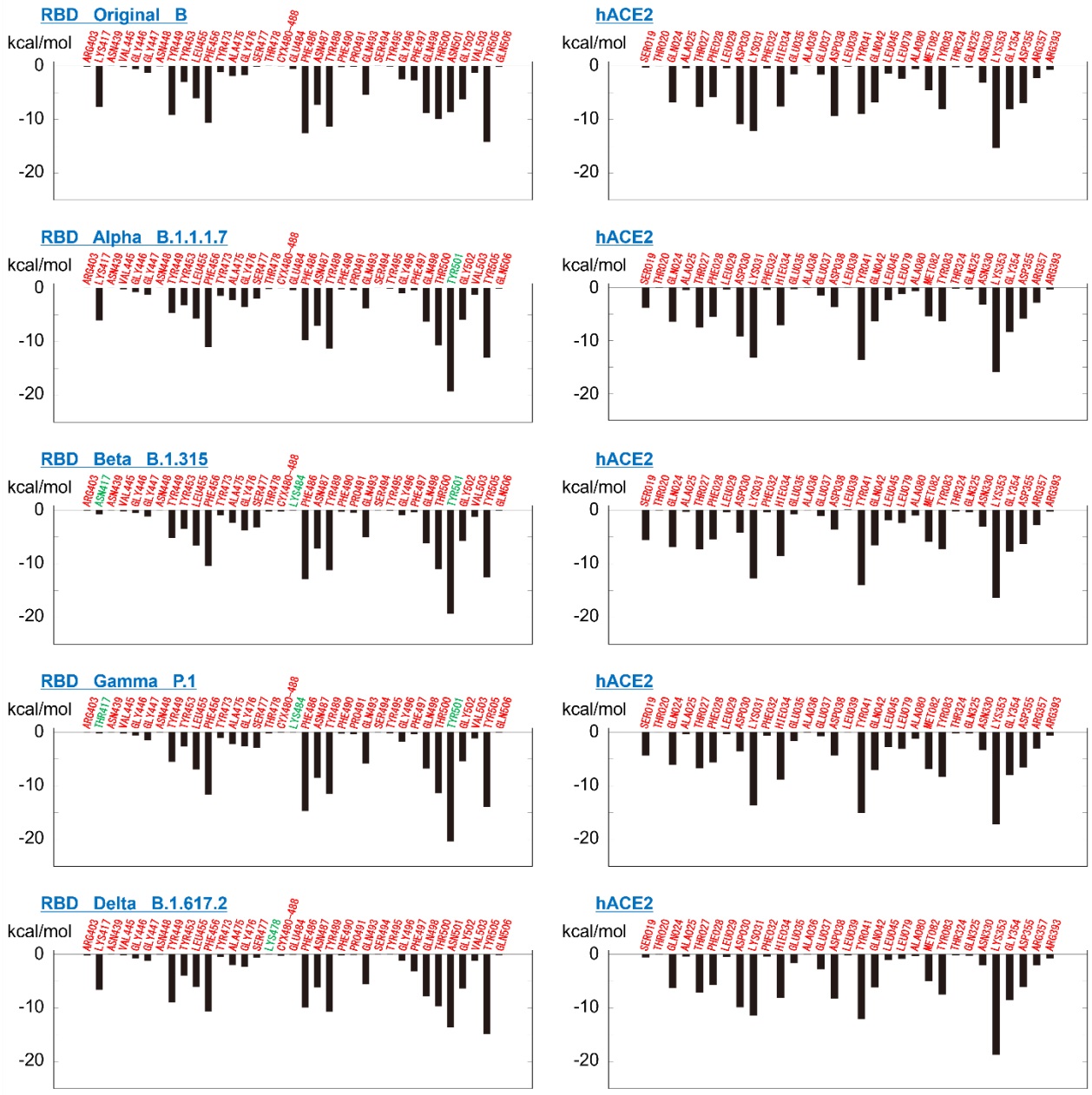

Figure S9(continue)

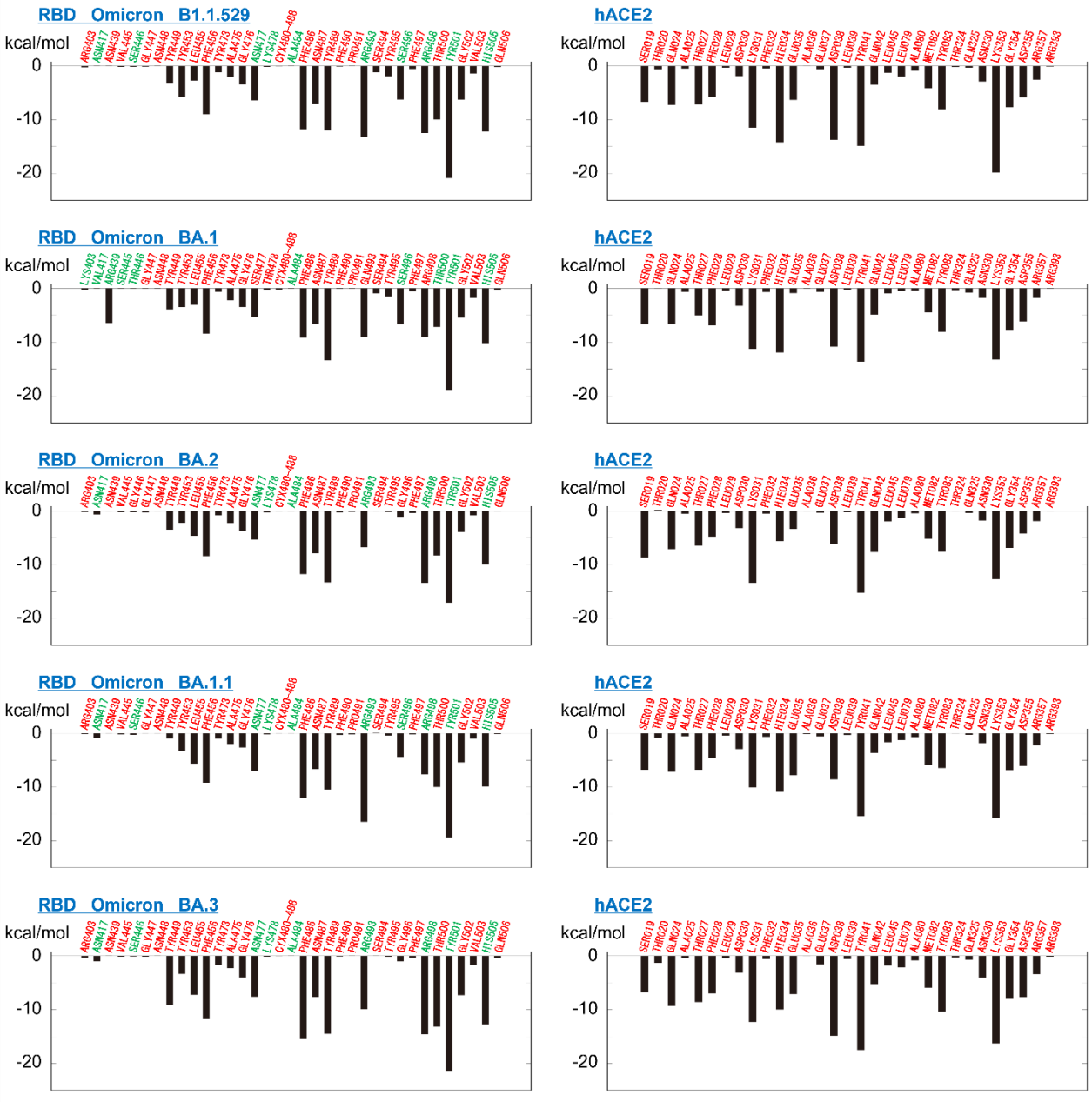

Figure S9 (continue)